ISSN 1855-9913
Journal of the Laser and Health Academy
Vol. 2017, No.1; www.laserandhealth.com

# Photoacoustic Endodontics Using the Novel SWEEPS Er:YAG Laser Modality

**Nejc Lukac[1], Blaz Tasic Muc[1], Matija Jezersek[1], Matjaz Lukac[2]**
*[1]University of Ljubljana, Faculty of Mechanical Engineering, Askerceva 6, 1000 Ljubljana, Slovenia*
*[2]Josef Stefan Institute, Jamova 39, 1000 Ljubljana, Slovenia*

## ABSTRACT

A new SWEEPS (Shock Wave Enhanced Emission Photoacoustic Streaming) modality for Er:YAG laser is presented, developed especially to improve the cleaning and disinfecting efficacy of laser-assisted endodontic procedures.

Typically, shock waves are not emitted during laser-assisted irrigation of spatially confined root canals. However, by using the new SWEEPS modality, an acceleration of the collapse of the laser-induced bubbles is achieved, leading to the emission of shock waves also into narrow root canals. The emitted primary shock waves that reach the smear layer at super-sonic speeds and the shear flows created by the fast collapse of secondary bubbles near the canal walls enhance the cleaning and disinfecting efficacy of laser-induced irrigation. With its precise delivery of shock waves into cleaning fluids and the resulting enhanced fluid dynamics, SWEEPS promises to represent an entirely new way of thinking about root canal therapy.

**Key words:** laser induced irrigation, laser endodontics, Er:YAG, photon induced photoacoustic streaming.

*Article: J. LA&HA, Vol. 2017, No.1; pp.01-07.*
*Received: February 15, 2017; Accepted April 15, 2017.*



## I. INTRODUCTION

The ability to clean, debride and disinfect dental root canals is limited by the complex anatomy of the dental root-canal system, and the limited penetration depth of commonly used irrigants into the dentine [1-6]. One of the main problems in endodontics is the non-turbulent fluid dynamics of irrigants in the confined canal space, which hinders deep penetration of the irrigant. Different agitation techniques have been introduced with the goal of improving the efficacy of irrigation solutions, including agitation with ultrasonic devices [7]. However, the effectiveness of this method has been found to be limited to the vicinity of the ultrasonic needle, which makes this method relatively ineffective [8]. In recent years an advanced photon-activated irrigation method has been introduced with a goal to overcome this problem [9-24]. This photon-induced photoacoustic streaming (PIPS) technique is based on placing a laser fiber tip into the pulp chamber filled with an irrigation fluid, and emitting a pulsed laser light into the fluid [13]. If the laser light is sufficiently absorbed by the fluid, the fluid is locally and instantly heated over its boiling point and a vapor bubble starts to develop at the fiber tip's end [8, 19, 24]. The vapor bubble first expands and then collapses after reaching its maximum volume. Under certain conditions the collapse initiates the growth of a second bubble. This turbulent photo-acoustic agitation of irrigants moves the fluid three-dimensionally throughout the root-canal system, actively pumps the tissue debris out of the canals, and is expected to clean and disinfect not only the main but also the lateral canals [21, 22, 24-26].

The clinical safety and efficacy of the PIPS irrigation technique has been investigated and confirmed by many studies [9-15, 22]. But a question arises of whether the efficacy of the technique can be improved even further. For example, it has been determined that, as opposed to large liquid reservoirs [19], shock waves, i.e., waves travelling faster than sound are not observed in spatially confined reservoirs such as root canals [8]. This is because in narrow canals cavitation dynamics is significantly slowed down by the friction on the canal walls and by the limited space available for the quick displacement of the liquid during the bubble's expansion and contraction. If the PIPS technique could be enhanced by the capability of generating shock waves in the root canal, this would result in shear flows capable of removing particles from the root canal surface. Additionally, since in the narrow root canal the emitted shock waves would reach the smear layer at supersonic speed, this could enhance the bactericidal effect of the technique and further increase its cleaning efficacy [34, 35].

In this paper, we report on a new SWEEPS (Shock Wave Enhanced Emission Photoacoustic Streaming) modality for Er:YAG laser developed especially to improve the cleaning and disinfecting efficacy of the photon-induced photoacoustic streaming procedure. The newly introduced SWEEPS modality resembles to some extent the technique used in extracorporeal shock-wave lithotripsy, where appropriately timed ultrasonic waves are utilized to effectively break kidney stones [27, 28].

## II. MATERIALS AND METHODS

The study was carried out on Er:YAG laser-induced cavitation dynamics in narrow hole models of a liquid-filled root canal. The Er:YAG system (λ = 2.94 μm) used was a LightWalker ATS (manufactured by Fotona d.o.o.), equipped with a contact fiber-tip handpiece H14.

Single laser pulses or pairs of individual pulses were delivered into liquid (distilled water). In the two-pulse experiments, the pulses were separated by a temporal delay (Tp). A series of measurements were conducted by varying Tp in the range of 200 to 800 μs in 1 μs intervals.

Two experimental set-ups were used to measure the cavitation characteristics. In the first experimental set-up, a block of acrylic glass with canals of varying diameters (1.5 – 6 mm) and lengths (10 -30 mm) was used to simulate various cavity dimensions. The block was submerged into a basin of distilled water and an Er:YAG laser fiber tip was positioned in the center of the cross-section of the hole. The oscillations of the cavitation bubbles were recorded using a high-speed camera (Photron, Fastcam, SA-Z) at 100,000 frames per second with an exposure time of 250 ns. Alternatively, a shadow-graphic setup described previously in [8, 24] was used. In this set-up, cavitation bubbles and shock waves were recorded using 30 ps long frequency-doubled Nd:YAG (λ = 532 nm) illumination pulses that were imaged through a microscope by a charge-coupled device (CCD) camera.

The second experimental set-up consisted of a laser beam deflection probe (LBDP) in a basic arrangement similar to the one used in [29]. A block of aluminum with canals of different diameters (2, 3, 6 and 8 mm) and a length of 25 mm was submerged in a reservoir of distilled water. The measuring system consisted of a He-Ne laser beam (λ = 633 nm) focused to a measuring spot 1 mm below the lower edge of the hole and centered on a quadrant photodiode (QPD). The refractive index gradient caused by the propagation of an Er:YAG laser-induced pressure wave through the water resulted in the deflection of the probe laser beam and consequently in the variation of the LBDP signal.

## III. RESULTS

### a) Measurements of shock waves in root canal models

Figure 1 shows an idealized temporal development of a bubble as observed experimentally following the emission of a single Er:YAG laser pulse through a fiber into a liquid-filled canal (with diameter *d* and length *L*) at time $T=T_0$.

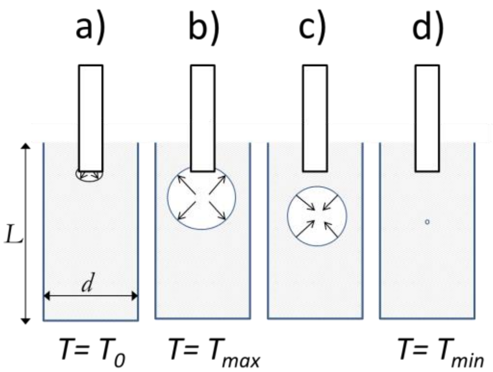


Fig. 1: Cavitation bubble oscillation sequence following the emission of a single Er:YAG laser pulse. A vapor bubble starts to expand when a laser pulse is emitted at $T=T_0$ (a) until the bubble reaches its maximum size at $T = T_{max}$ (b), after which the bubble starts to collapse (c) until it reaches its minimal size at $T = T_{min}$ (d) and rebounds. In narrow root-canal like reservoirs, the bubble collapse is too slow to result in the emission of shock waves.

When a pulsed Er:YAG laser beam is delivered to a liquid at a time $T= T_0$, a bubble oscillation sequence develops. In the 1st phase of the bubble oscillation sequence (from time $T_0$ to time $T_{max}$), laser energy deposition into the liquid via absorption causes superheating of the liquid, and boiling induces a vapor bubble. The vapor bubble expands rapidly and thereafter reaches its maximum size at $T_{max}$. In the 2nd phase (from time $T_{max}$ to time $T_{min}$), the difference in pressures forces the vapor bubble to collapse. During the collapse, a portion of the energy stored in the vapor bubble is converted into acoustic energy.

When the bubble collapse is sufficiently fast, shock waves are emitted by the end of the 2nd phase. Experiments have shown that the collapse of the Er:YAG laser-generated bubble leads to shock wave emission only in very large liquid reservoirs [19], while in narrow reservoirs such as liquid-filled root canals the emission of shock waves is not observed [8]. This is due to the slower cavitation dynamics, resulting in longer bubble oscillation periods ($T_{osc} = T_{min} - T_0$) in narrow canals. Longer bubble oscillation times are attributed to the friction on the canal walls and to the limited space available for the rapid fluid displacement during the bubble's expansion and contraction.

The measured dependence of the oscillation period $T_{osc}$ on the canal diameter is shown in Fig. 2. As can be seen from Fig. 2, the bubble oscillation is more than two-times slower in a 2 mm cavity ($T_{osc} \approx 640$ μs) in comparison to that in an infinite reservoir ($T_{osc} \approx 300$ μs).

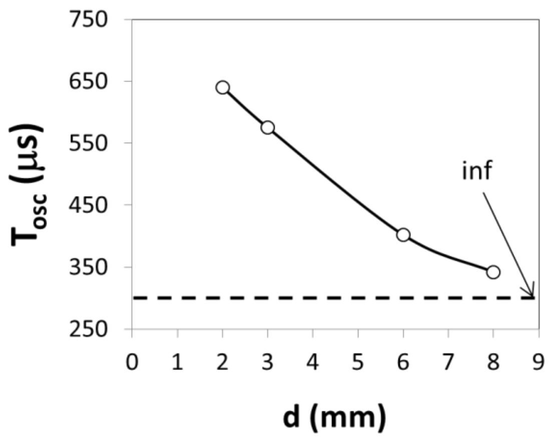


Fig. 2: Measured dependence of the bubble oscillation period $T_{osc}$ on the diameter of the canal, for laser pulse energy of 20 mJ. The dotted line represents $T_{osc}$ in an infinite reservoir.

There is another important difference between laser-induced cavitation dynamics in infinite and spatially confined reservoirs. In spatially limited canals, secondary smaller bubbles are formed throughout the canal in addition to the larger initial bubble (See Fig. 3).

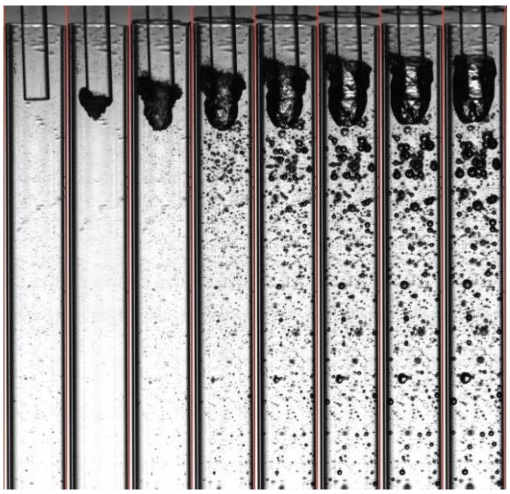

Fig. 3: High-speed camera temporal sequence of images of the development of an initial bubble close to the fiber tip, accompanied by smaller secondary bubbles forming throughout the blind canal, as observed following the emission of a single laser pulse. Time increment between images is 40 μs.

Provided that a violent collapse of the initial and secondary bubbles could be produced, this would result in the emission of a large number of shock waves throughout the canal, potentially significantly increasing the cleaning and disinfecting efficacy of laser-induced irrigation.

In the study, an innovative technique was developed in order to accelerate the bubble collapse and consequently <u>to generate shock waves also in spatially confined reservoirs, such as root canals</u>. This SWEEPS (Shock Wave Enhanced Emission Photoacoustic Streaming) technique consists of delivering a subsequent laser pulse into the liquid at an optimal time $T_{opt}$ when the initial bubble is in the final phase of its collapse (see Fig. 4). The growth of the subsequent bubble exerts pressure on the collapsing initial bubble, accelerating its collapse and the collapse of secondary bubbles, resulting in the emission of primary and also secondary shock waves.

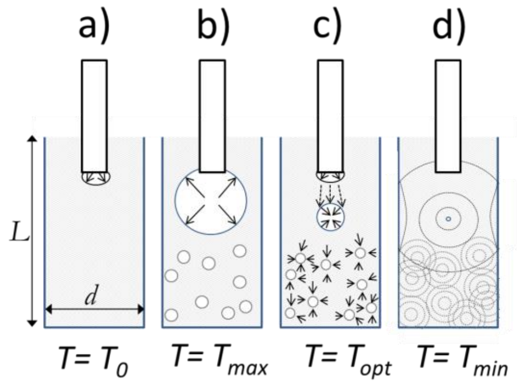


Fig. 4: Cavitation bubble dynamics sequence during and following the emission of a SWEEPS laser pulse pair. A vapor bubble starts to develop at the fiber tip's end, following the emission of the initial laser pulse (a). The initial vapor bubble first expands together with accompanying smaller secondary bubbles, until it reaches its maximum volume (b). During the initial bubble's collapse a subsequent vapor bubble starts to grow following the emission of the subsequent laser pulse (c). When the growth of the subsequent bubble is properly timed, the pressure waves caused by the subsequent bubble force the initial bubble and secondary bubbles into a violent collapse, resulting in the emission of shock waves (d).

The optimal time $T_{opt}$, was found experimentally to be approximately equal to $T_{opt} \approx 0.9\ T_{osc}$, with the FWHM of the optimal region of approximately 50 μs.

The observed shock waves in a narrow canal, using the SWEEPS laser pulse pair of two individual laser pulses separated by the optimal temporal separation $T_p = T_{opt}$, are shown in Fig. 5.

Figure 5a shows shadow-graphic images of detected shock waves being emitted during the collapse of an initial cavitation bubble, accelerated by the beginning growth of the subsequent bubble which can be seen forming at the bottom of the fiber tip. The violent collapse of the initial bubble also leads to the collapse of smaller secondary bubbles forming alongside the entire canal, which also emit shock waves when they collapse (Fig. 5 b).

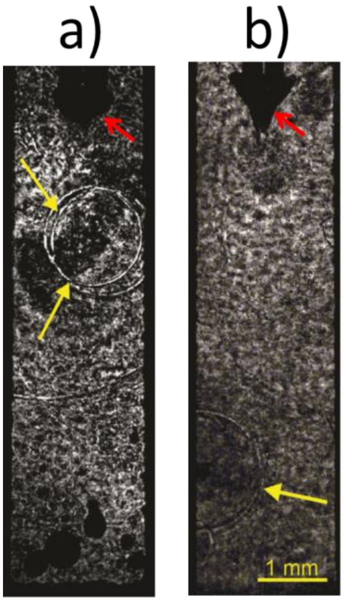


Fig. 5: a) Primary shock wave emission following the SWEEPS-accelerated collapse of the initial bubble; b) Secondary shock waves are also emitted along the wall canals as a result of the collapse of secondary bubbles, which are generated deeper in the canal during the initial bubble's growth and collapse. Yellow (long) arrows point to the emitted shock waves and red (short) arrows show the growing bubble of the subsequent laser pulse.

The amplification of photoacoustic streaming by the SWEEPS technique was also demonstrated by measuring the generated pressure waves using a laser beam deflection probe (LBDP). The pressure waves produced by the shock wave-enhancing SWEEPS technique were observed to result in an amplified LBDP signal when compared to that produced by the standard PIPS technique. The measured amplification factor $A_f$, as a function of the canal diameter, is shown in Fig. 6, for a flat fiber and individual laser pulse energy of 20 mJ. In narrow canals with diameters < 4 mm, where the acceleration of the bubble collapse is largest in comparison to the speed of collapse in an infinite reservoir, the LBDP pressure wave signals are increased by a factor of $A_f \approx 2$.

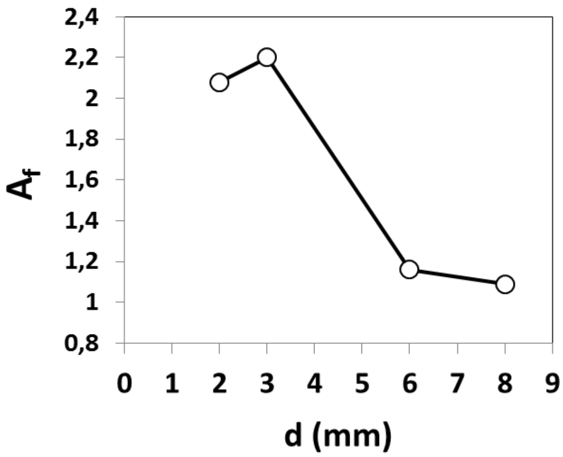


Fig. 6: The factor of increase in the LBDP amplitude of pressure waves generated by the SWEEPS technique, in comparison to the pressure waves generated by the standard PIPS technique. The amplification is strongest in narrow canals where the acceleration of the bubble collapse is largest in comparison to the speed of collapse in an infinite reservoir. The line is a visual aid only.

It is important to note that the observed amplification could not be achieved by simply increasing the initial laser pulse energy. This can be seen in Fig. 7, which shows the dependence of the pressure amplitude (the LBDP signal) on the individual laser pulse energy for a flat (Varian) and conical (PIPS) tip under single-pulse and SWEEPS conditions. The measured single-pulse LBDP signal is approximately independent of the laser pulse energy. This is because higher laser energy results in an increase in the size of the cavitation bubble relative to the dimensions of the spatially limited root canal, which leads to prolonged bubble oscillation times at higher laser energies.

However, as shown in Fig. 7 when a SWEEPS pair is emitted with an optimal delay time, the pressure waves, resulting from the collapse of the initial bubble become significantly amplified. It is to be noted that the actual amplification of pressure waves higher in the canal, where the collapsing bubble is located, is expected to be much higher than what was measured at a distance of approximately 25 mm below the bubble (Fig. 6). The shock waves are emitted at shock speeds close to the collapsing bubble, but become considerably slower as they travel 25 mm deep into the canal where the measurement was made. In spite of this slowing down effect, the pressure waves were still measured to be approximately two-times stronger under SWEEPS conditions.

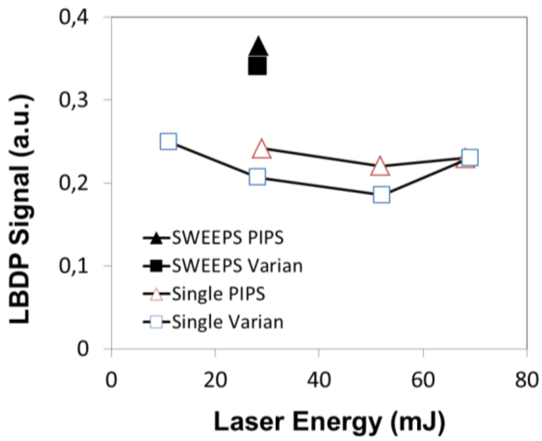


Fig. 7: Measured dependence of the pressure amplitude (LBDP signal) following the collapse of the initial bubble on the individual laser pulse energy for a flat (Varian) and conical (PIPS) tip under single pulse and SWEEPS conditions, for a 6 mm diameter canal.

**b) Auto SWEEPS Er:YAG laser modality**

When considering the use of the SWEEPS technique in clinical practice, it is important to take into account that the root canal diameter varies from tooth to tooth and also along the length of the root canal. In addition, $T_{opt}$ would to a certain degree depend also on whether the practitioner positions the fiber tip exactly at the center or closer to the walls of the root canal. Therefore, a two-pulse laser emission with a fixed temporal separation $T_p$ requires from the practitioner to adjust the SWEEPS separation $T_p$ to the diameter of the treated cavity in order to obtain consistent shock wave emission.

For this reason, a special Auto SWEEPS Er:YAG laser modality was developed, where the temporal separation between the pair of laser pulses is continuously swept back and forth in 10 μs steps between $T_p$ = 300 μs and $T_p$ = 650 μs. This ensures that during each sweeping cycle there is always at least a 50 μs wide temporal separation range when pulses are separated by $T_p \approx T_{opt}$, as required for shock wave emission. The sweeping modality also ensures that the optimal conditions are approximately reached along the length of the canal by matching the changing diameter conditions during the Auto SWEEPS cycle. The Auto SWEEPS modality also eliminates the need for the operator to precisely position the fiber tip in the center of the cross-section of the root canal.

Figure 8 shows images of photoacoustic streaming in a root canal model for three stages during an Auto SWEEPS cycle: a) $T_p > T_{opt}$; b) $T_p \approx T_{opt}$ and c) $T_p < T_{opt}$. The Er:YAG laser system used was an ASP (Adaptive Structured Pulse) powered LightWalker ATS (manufactured by Fotona).

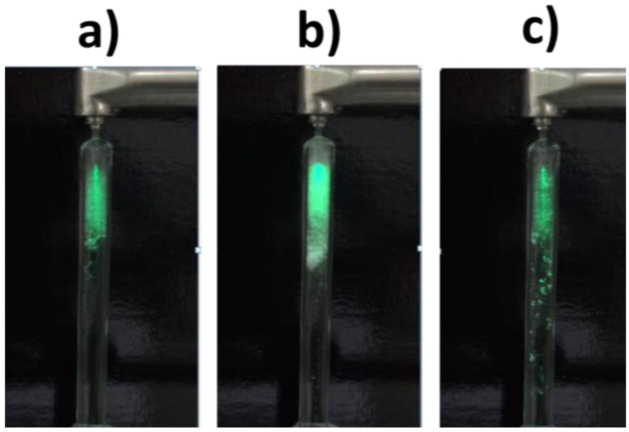


Fig. 8: Images of cavitation bubbles during an Auto SWEEPS cycle as the temporal separation between the SWEEPS laser pulse pair is being swept from a) long separations ($T_p > T_{opt}$) to c) short separations ($T_p < T_{opt}$ ). Fig 7 (b) shows formation of cavitation bubbles when the pulse separation approached the optimal separation, $T_p \approx T_{opt}$.

As can be seen from Fig. 8, the Auto SWEEPS "sweeping" modality has an additional beneficial effect on the irrigation efficacy, in addition to the generation of shock waves. By sweeping the separation of SWEEPS pulse pairs, the photoacoustic streaming is being swept locally from a spatial region close to the fiber tip when $T_p > T_{opt}$ (Figure 7a), to deeper into the root canal when $T_p < T_{opt}$ (Figure 7c). When, for example, $T_p < T_{opt}$, the subsequent bubble from the subsequent laser pulse effectively "propels" the initial bubble deeper into the canal, thus effectively improving the irrigation effect deeper within the canal. This effect can be observed in more detail in high-speed camera images of the bubble dynamics during a SWEEPS laser pair emission for $T_p < T_{opt}$ (Fig. 9).

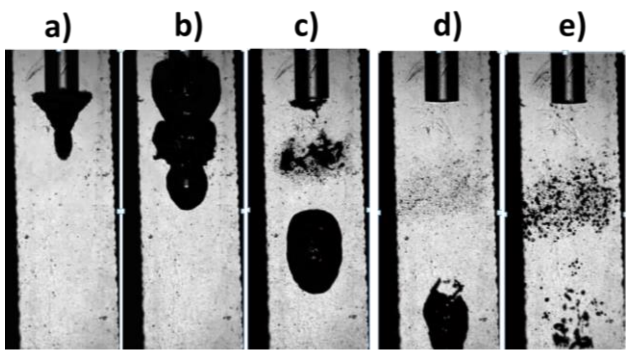


Fig. 9: Sequence of images showing the development of cavitation bubbles during an Auto SWEEPS cycle for the laser pulse separation of $T_p < T_{opt}$. A subsequent bubble forming very quickly following the initial bubble is shown in Figs a) and b). The bubble's "propulsion" deeper into the canal can be seen in Figs c) and d).

For comparison, high speed camera images of the bubble dynamics during a standard PIPS single-pulse emission is shown in Fig.10. In this case, the bubble cavitation is located predominantly only near the conical PIPS fiber tip.

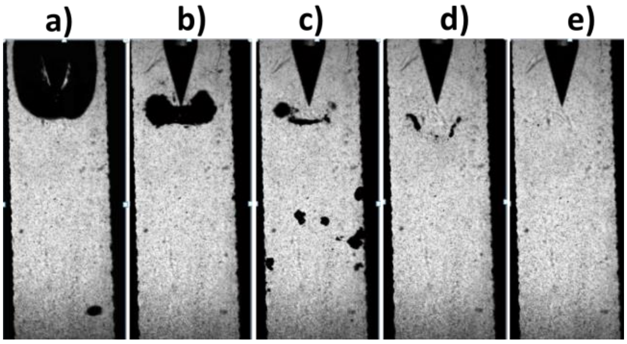


Fig. 10: Sequence of images showing the development of a cavitation bubble following a single PIPS Er:YAG laser pulse. The bubble cavitation is located predominantly close to the conical PIPS fiber tip.

## IV. DISCUSSION

In spatially confined reservoirs such as root canals, cavitation pressure waves cannot be increased, or shock waves generated, by simply increasing the energy of a single PIPS Er:YAG laser pulse. As measurements have demonstrated, an increase in the PIPS laser pulse energy within the range of laser pulse energies from 10 – 50 mJ, actually results in a lower amplitude of the LBDP pressure wave signal. This is due to an increase in the size of the cavitation bubble relative to the dimensions of the canal, which leads to slowed down bubble oscillation dynamics at higher laser energies. It is only by optimally shaping the laser pulse emission temporally using the SWEEPS technique that we were able to achieve the amplification of the photoacoustic streaming effects.

It is also worth noting that when a standard conical tip (Fotona PIPS) was used in our experiments, the cone of the tip became damaged following a single optimally separated SWEEPS laser pulse pair, demonstrating the strength of the created shock waves. For this reason, a special fiber tip (SWEEPS 600 by Fotona) is recommended to be used for performing SWEEPS endodontic treatments.

A preliminary study of the potential apical irrigant extrusion during the SWEEPS laser irrigation has also been carried out [30]. Irrigation using two standard endodontic irrigation needles (notched open-end and side-vented) was compared with the PIPS and SWEEPS laser irrigation procedures. Both the PIPS and SWEEPS irrigation procedures resulted in a significantly lower apical extrusion compared to the conventional irrigation with endodontic irrigation needles, in agreement with a previous report [31].

Generating SWEEPS laser pulse pairs with equal individual pulse energies during the SWEEPS cycle represents a significant technological challenge. This is because the lasing efficiency of each of the laser pulses in the pulse pair changes continuously during the SWEEPS cycle. For this reason, the recently introduced 3rd generation Fotona ASP (Adaptive Structured Pulse) power generation technology [32] was used to generate the new SWEEPS modality. The same ASP technology has also been used lately to optimize the performance of the Er:YAG laser's QSP (Quantum Square Pulse) mode with regard to critical requirements for minimally invasive laser dentistry [32, 33].

## V. CONCLUSIONS

When performing laser-activated PIPS endodontics, it is desirable to be able to increase the speed of generated waves in irrigants, with a goal to not only turbulently spread irrigants throughout the root canal system, but also to directly remove the smear layer and disinfect the root canal walls [34, 35].

In spatially confined root canals, single laser pulses do not result in the emission of shock waves in laser-irradiated irrigants. Additionally, the effectiveness of pressure waves cannot be increased by increasing the laser pulse energy. However, as shown by our study, enhanced pressure waves travelling at shock speeds can be created in root canals during laser endodontic procedures using the new SWEEPS (Shock Wave Enhanced Emission Photoacoustic Streaming) Er:YAG laser modality.

In conclusion, SWEEPS delivers precise concentration of shock waves into cleaning fluids, reaching deep into lateral canals and microscopic tubules to remove tissue, debris, biofilm and bacteria. This new modality thus promises to significantly enhance the efficacy of the standard PIPS (Photon Induced Photoacoustic Streaming) laser-induced irrigation procedures

## ACKNOWLEDGMENT

The authors wish to thank Fotona (www.fotona.com) for providing the laser systems used in this research. The authors acknowledge financial support from the state budget of the Slovenian Research Agency and Fotona. Three of the authors (Lukac Nejc, Tasic Muc Blaz and Lukac Matjaz) are currently also employees of Fotona.

## REFERENCES


1. Vertucci F, Seelig A, Gillis R. Root canal morphology of the human maxillary second premolar. Oral Surg Oral Med Oral Pathol. 1974;38(3):456-64.
2. Peters OA, Peters CI, Basrani B. Cleaning and shaping the root canal system (Chapter 6) In: Hargreaves KM, Bermann LH. Cohen's Pathways of the Pulp 2016 11th edn Elsevier 209-279.
3. Baumgartner JC. Endodontic Microbiology. Walton RE, Torabinejad M. Principles and practice of endodontics. 1996; 2nd Edition, Chapt 16 :277-291.
4. McComb D, Smith DC. A preliminary scanning electron microscopic study of root canals after endodontic procedures. J Endod. 1975;1(7):238-42.
5. Fairbourn DR, McWalter GM, Montgomery S. The effect of four preparation techniques on the amount of apically extruded debris. J Endod. 1987;13(3):102-8.
6. Mader CL, Baumgartner JC, Peters DD. Scanning electron microscopic investigation of the smeared layer on root canal walls. J Endod. 1984;10(10):477-83.
7. Cameron JA. The use of ultrasound for the removal of the smear layer. The effect of sodium hypochlorite concentration; SEM study. Australian Dental Journal. 1988;33(3):193-200.
8. Lukac N, Gregorcic P, Jezersek M. Optodynamic Phenomena During Laser-Activated Irrigation Within Root Canals. International Journal of Thermophysics. 2016;37(7):1-8.
9. Blanken J, De Moor RJ, Meire M, Verdaasdonk R. Laser induced explosive vapor and cavitation resulting in effective irrigation of the root canal. Part 1: a visualization study. Lasers Surg Med. 2009;41(7):514-9.
10. Gentil RJ et al. Laser induced explosive vapor and cavitation resulting in effective irrigation of the root canal. Part 2: Evaluation of the efficacy. Lasers Surg Med 2009; 41(7): 520-523.
11. Kuhn K, Rudolph H, Luthardt RG, Stock K, Diebolder R, Hibst R. Er:YAG laser activation of sodium hypochlorite for root canal soft tissue dissolution. Lasers Surg Med. 2013;45(5):339-44.
12. Peters OA, Bardsley S, Fong J, Pandher G, Divito E. Disinfection of root canals with photon-initiated photoacoustic streaming. J Endod. 2011;37(7):1008-12.
13. DiVito E, Peters OA, Olivi G. Effectiveness of the erbium:YAG laser and new design radial and stripped tips in removing the smear layer after root canal instrumentation. Lasers Med Sci. 2012;27(2):273-80.
14. Olivi G, DiVito EM. Photoacoustic Endodontics using PIPS™: experimental background and clinical protocol. J LA&HA- J. Laser Health Acad 2012; 2012(1):22-25.
15. Deleu E, Meire MA, De Moor RJ. Efficacy of laser-based irrigant activation methods in removing debris from simulated root canal irregularities. Lasers Med Sci. 2015;30(2):831-5.
16. Hale GM, Querry MR. Optical Constants of Water in the 200-nm to 200-microm Wavelength Region. Appl Opt. 1973;12(3):555-63.
17. Matsumoto H, Yoshimine Y, Akamine A. Visualization of irrigant flow and cavitation induced by Er:YAG laser within a root canal model. J Endod. 2011;37(6):839-43.
18. Vogel A, Venugopalan V. Mechanisms of pulsed laser ablation of biological tissues. Chem Rev. 2003;103(2):577-644.
19. Gregorcic P, Jezersek M, Mozina J.Optodynamic energy-conversion efficiency during an Er:YAG-laser pulse delivery into a liquid through different fiber-tip geometries. J Biomed Opt 2012 Jul;17(7): 075006.
20. Lloyd A, Uhles JP, Clement DJ, Garcia-Godoy F. Elimination of intracanal tissue and debris through a novel laser-activated system assessed using high-resolution micro-computed tomography: a pilot study. J Endod. 2014;40(4):584-7.
21. Koch JD, Jaramillo DE, DiVito E, Peters OA. Irrigant flow during photon-induced photoacoustic streaming (PIPS) using Particle Image Velocimetry (PIV). Clin Oral Investig. 2016 Mar;20(2):381-6.
22. Arslan H, Akcay M, Ertas H, Capar ID, Saygili G, Mese M. Effect of PIPS technique at different power settings on irrigating solution extrusion. Lasers Med Sci. 2015;30(6):1641-5.
23. Gregorcic P, Lukac N, Mozina J, Jezersek M. In vitro study of the erbium:yttrium aluminum garnet laser cleaning of root canal by the use of shadow photography. J. Biomed. Opt. 2016, 21: 015008.
24. Lukac N, Zadravec J, Gregorcic P, Lukac M, Jezersek M, Wavelength dependence of photon-induced photo-acoustic streaming technique for root canal irrigation, J Biomed Opt, 2016.
25. Ackay M, Arslan H, Durmus N, Mese Merve, Davut Capar I, Dential tubule penetration of AH Plus, iRoot SP, MTA Fillapex, and GuttaFlow Bioseal root canal sealers after different final irrigation procedures: a confocal microscopic study, Lasers Surg Med 2016; 48: 70-76.
26. Mir M, Gutknecht N, Poprawe R, Vanweersch L, Lampert F, Visualising the procedures in the influence of water on the ablation of dental hard tissue with erbium: yttrium–aluminium–garnet and erbium, chromium: yttrium–scandium–gallium-garnet laser pulses, Lasers in Med Sci 2009, 24(3): 365-374.
27. De Icaza-Herrera M, Fernandez F, Loske AM. Combined short and long-delay tandem shock waves to improve shock wave lithotripsy according to the Gilmore-Akulichev theory. Ultrasonics. 2015;58:53-9.
28. Loske AM, Prieto FE, Fernandez F, van Cauwelaert J. Tandem shock wave cavitation enhancement for extracorporeal lithotripsy. Physics in medicine and biology. 2002;47(22):3945-57.
29. Gegorcic P, Petkovsek R, Mozina J, Mocnik G, Measurements of cavitation bubble dynamics based on a beam-deflection probe, Appl Phys 2008, 93(4): 901-905.
30. Jezersek M, Pirnat L, Jereb T, Lukac N, Tenyi A, Fidler A, Measurement of apical extrusion during laser activated irrigation within root canals using particle image velocimetry (PIV). COLA 2017 -International Conference on Laser Ablation.
31. Snjaric D, Apical Irrigant Extrusion during Laser-Activated Irrigation Compared to Conventional Endodontic Irrigation Regimens - Preliminary Study Results, J. LA&HA - J. Laser Health Acad 2016; 2016(1): 54.
32. Lukac N, Lukac M, Jezersek M, QSP Mode Characteristics of 3rd Generation ASP Powered Er:YAG Dental Lasers, J. LA&HA - J. Laser Health Acad 2016; 2016(1): 1-5.
33. Lukac N, Suhovrsnik T, Lukac M, Jezersek M, Ablation characteristics of quantum square pulse mode dental erbium laser. Journal of biomedical optics, 2016, vol. 21 (1): 1-10.
34. Wu H, Liu SC, Effect of Supersonic Waves on Bacteria, Proc. Soc. Exp. Biol. Med. 1931, vol. 28: 782-784.
35. Furuta M, Yamaguchi M, Tsukamoto T, Yim B, Stavarache CE, Hasiba K, Maeda Y. Inactivation of Escherichia coli by ultrasonic irradiation, Ultrason Sonochem. 2004 Apr;11(2):57-60.